
Masters Theses

Student Theses and Dissertations

1973

Model correction for the formation of amorphous silicon by ion implantation

John Robert Dennis

Follow this and additional works at: https://scholarsmine.mst.edu/masters_theses



Part of the [Physics Commons](#)

Department:

Recommended Citation

Dennis, John Robert, "Model correction for the formation of amorphous silicon by ion implantation" (1973). *Masters Theses*. 3513.

https://scholarsmine.mst.edu/masters_theses/3513

This thesis is brought to you by Scholars' Mine, a service of the Missouri S&T Library and Learning Resources. This work is protected by U. S. Copyright Law. Unauthorized use including reproduction for redistribution requires the permission of the copyright holder. For more information, please contact scholarsmine@mst.edu.

MODEL CORRECTION FOR THE FORMATION OF
AMORPHOUS SILICON BY ION IMPLANTATION

BY

JOHN ROBERT DENNIS, 1943-

A THESIS

Presented to the Faculty of the Graduate School of the

UNIVERSITY OF MISSOURI-ROLLA

In Partial Fulfillment of the Requirements for the Degree

MASTER OF SCIENCE IN PHYSICS

1973

Approved by

T2854
31 pages
c.1

Edward B. Hale (Advisor)

Robert Gerson

W. J. James

ABSTRACT

ESR has been used to study the formation of an amorphous layer in silicon by ion implantation. The room temperature implants were done at 20 keV with low dose rates. The critical dose was determined as a function of ion mass for six different ion species. Our experimental heavy ion results agree with those found by other ESR investigators at higher energy, but are not the same for light ions. However, our light and heavy ion results agree with electron microscope measurements for low energy implants. An energy-independent model for the formation of amorphous silicon by ion implantation has been used to explain previous results. An energy-dependent model has been developed by incorporating energy dependent range corrections. The results of all three independent experiments can be explained by the new model.

ACKNOWLEDGMENTS

I wish to express my appreciation and thanks to Dr. Edward Hale for contributing both time and ideas which helped make this project successful. Also, I would like to acknowledge the financial support of the Air Force Office of Scientific Research, AFSC and the National Science Foundation.

TABLE OF CONTENTS

	Page
ABSTRACT.....	ii
ACKNOWLEDGMENT.....	iii
LIST OF ILLUSTRATIONS.....	v
LIST OF TABLES.....	vi
I. INTRODUCTION.....	1
II. REVIEW OF LITERATURE.....	3
III. EXPERIMENTAL METHODS.....	7
IV. EXPERIMENTAL RESULTS AND DISCUSSION.....	9
V. CONCLUSIONS.....	11
BIBLIOGRAPHY.....	23
VITA.....	25

LIST OF ILLUSTRATIONS

Figures	Page
1. Plot on log-log scale of relative ESR signal amplitude as a function of ion dose for 20 keV N^+ ions implanted in silicon.....	15
2. Plot on log-log scale of relative ESR signal amplitude as a function of ion dose for 20 keV N_2^+ ions implanted in silicon.....	16
3. Plot on log-log scale of relative ESR signal amplitude as a function of ion dose for 20 keV Ne^+ ions implanted in silicon.....	17
4. Plot on log-log scale of relative ESR signal amplitude as a function of ion dose for 20 keV Ar^+ ions implanted in silicon.....	18
5. Plot on log-log scale of relative ESR signal amplitude as a function of ion dose for 20 keV Kr^+ ions implanted in silicon.....	19
6. Plot on log-log scale of relative ESR signal amplitude as a function of ion dose for 20 keV Xe^+ ions implanted in silicon.....	20
7. Plot of critical dose at 300°K as a function of atomic number of ion.....	21

LIST OF TABLES

Table	Page
I. Experimentally determined critical dose values for various ions and energies for room temperature implants.....	22

I. INTRODUCTION

Ion implantation of semiconductors has been an area of great interest for the last several years. This interest has come about because of the potential advantages of using ion implantation as a doping technique in the production of semiconductor devices rather than the conventional diffusion methods which have been used in the past.

It has been found that, if an amorphous layer is formed by the ion implantation, the implanted dopant can then often be introduced into electrically active lattice sites by annealing at a relatively low temperature ($\approx 600^{\circ}\text{C}$).¹⁻³ On the other hand, if a continuous amorphous layer is not formed by the ion implantation, then the recrystallization of the sample by annealing results in randomly oriented crystallites in the damaged region.

Because of the desirable effects of producing a continuous amorphous layer by the ion implantation, investigation of the formation of such a layer in silicon was chosen as a research project. The formation of a continuous amorphous layer in silicon was studied using ions of various mass. Silicon was chosen for this study because considerable experimental data on ion implantation in silicon are available in the literature. Furthermore, various aspects of crystalline silicon and of amorphous silicon have been studied previously using electron spin resonance, which was also to be used as a tool in this investigation. Another reason

for the choice of silicon was the existence in the literature of a model for the formation of a continuous amorphous layer in silicon by ion implantation.⁴

II. LITERATURE REVIEW

Most of the early work in ion implantation was focused on semiconductor devices. In 1953 Ohl⁵ reported improvements in the electrical properties of silicon point contact diodes by bombardment of the surface with various ions. Although some device oriented papers were published between 1952 and 1962⁶⁻⁹, it was not until the work of McCalden and Widmer¹⁰ in 1963 that interest in ion implantation of semiconductors was stimulated (see Gibbons, reference 1, for a brief summary of the preceding papers).

In his review paper in 1968 Gibbons divided ion implantation research into four principal topics. These topics were: "1) range-energy relations for the implanted ions; 2) crystalline sites and energy levels of the implanted ions; 3) structural and electrical effects of implantation-produced damage and its annealing behavior; and 4) device fabrication and characterization." Because of the large number of papers in ion implantation since 1963, only those papers dealing with the production of amorphous regions due to ion implantation will be considered. For a review of other aspects of ion implantation the reader is referred to Gibbons^{1,2} and to Mayor, et al.³

In 1965 J.R. Parsons¹¹ reported on the size and structure of the damaged regions in crystalline germanium created by 100 keV O⁺ ions. The implantations were done at 30°K and at room temperature. The bombarded samples were

examined under an electron microscope and it was found that an amorphous region was created surrounding the ion track. It was further noted that the area of this region normal to the surface was not the same for the 30°K implants as it was for the room temperature implants. It was also observed that as the dose was increased to 2×10^{15} ions/cm² that the entire surface region made a transition from crystalline to amorphous structure.

Then, in 1967 Davies, et al¹² studied the disorder produced by 40 keV Sb⁺ ions for room temperature implants in silicon, using He⁺ back-scattering techniques. When the amount of disorder created was plotted as a function of the dose in ions/cm², it was observed that a slope change occurred at about 1×10^{14} ions/cm². For larger doses the amount of disorder remained fairly constant. Davies, et al interpreted this to mean that at a dose of 1×10^{14} Sb⁺ ions/cm², an essentially continuous amorphous layer had been formed. In a later paper¹³ they repeated the experiment for Ga⁺ and P⁺ 40 keV ions in silicon, and for 40 keV In⁺ ions in germanium. The same conclusions were reached, with the critical dose for an amorphous layer as $\approx 7 \times 10^{14}$ P⁺ ions/cm² and 1×10^{14} Ga⁺ ions/cm² in silicon, and $\approx 7 \times 10^{13}$ In⁺ ions/cm² in germanium.

In the past, electron spin resonance has proved to be a very useful tool for the study of individual defects created by neutron irradiation. Also it has been very valuable for studying lattice location and electrical

activity of impurity atoms in the lattice, especially in silicon. Much work has been done in this area and a large number of point defects have been found and characterized. Because of the usefulness of ESR as a tool in studying point defects and lattice locations of impurities, it was applied to the study of ion implanted samples. From the middle 1960's to the present several papers have been published on the results of such investigations.¹⁴⁻²²

M.H. Brodsky and R.S. Title in 1969 reported the measurement and identification of ESR signals in thin films of amorphous silicon, germanium, and silicon carbide.²³ For silicon the linewidth of the ESR signal was 7.5 gauss at room temperature and narrowed to 4.7 gauss at 77°K. The line shape was Lorentzian and had an isotropic g value of 2.0055 ± 0.0005 . In a later paper Crowder, Title, Brodsky, and Pettit reported the detection by ESR of amorphous silicon created by ion implantation.²⁴ The ESR signals from the implanted samples had approximately the same linewidth and had the same g value as those from amorphous films. Their implantations were done with 280 keV P⁺ and As⁺ ions at room temperature. They further found that, as the dose in ions/cm² was increased, an abrupt change in the slope of the log of the ESR signal intensity versus the log of the ion dose occurred. This was interpreted as being the onset of a continuous amorphous layer. For 280 keV As⁺ ions, this change in slope occurred at approximately 3×10^{14} ions/cm², and for P⁺ ions, at approximately

1×10^{15} ions/cm². An energy independent model for the formation of amorphous silicon by ion implantation at all implant temperatures was then formulated by Morehead and Crowder.⁴ This model is of substantial importance in this research and is derived in Section V.

III. EXPERIMENTAL METHODS

The ion implantations were done at room temperature, 20 keV, and low dose rates ($\leq .25 \mu$ amperes/cm²) on a low energy Cockcraft-Walton ion accelerator.* The samples were undoped (≈ 500 ohm-cm) silicon wafers which were cut to approximately $\frac{1}{4}$ " x 1". The samples were then etched in CP4 solution (HNO₃, HF, and CH₃COOH in the ratios 5:3:3) to clean the surface and to remove any oxide layer. The samples were then mounted on the sample holder with copper print to insure good electrical contact and placed in the bombarding chamber. The samples were masked to expose a one cm² area to the ion beam. The ion beam was rastered by horizontal and vertical deflection plates, each driven with an amplified triangular waveform to obtain uniform beam coverage of the implanted area. A suppression grid was also used to avoid erroneous current readings due to secondary electrons. The dose in ions/cm² was determined as the product of the ion current, as measured on the sample, and the implant time.

The samples were examined by a Varian Model 4502 spectrometer in a Varian V-4531 Multi-purpose Cavity. The klystron was operated in the 100 kHz modulation mode at room temperature. The samples were all run under the same conditions and the relative signal amplitude was determined

*See the Masters Thesis of Gary Woodward, submitted in the Spring of 1973 for accelerator details.

by comparison with a ruby standard sample glued onto the cavity wall. Some samples were also examined using different spectrometer settings to insure that no saturation or passage effects were occurring.

IV. EXPERIMENTAL RESULTS AND DISCUSSION

A series of samples of varying doses for six different ions were prepared. The ions used were N^+ , N_2^+ , Ne^+ , Ar^+ , Kr^+ , and Xe^+ . The samples were examined on the ESR spectrometer, and a graph of the log of the relative signal amplitude versus the log of the ion dose in ions/cm² was plotted (see Figures 1-6). The critical dose was determined from the experimental plots as the intersection of the straight line extrapolations of the two distinctly different slopes (see Figure 1). The results of these determinations are listed in Table I. The critical dose for N_2^+ , which is not listed in Table I, was found to be 1.5×10^{15} ions/cm².

Some quantitative remarks can be made concerning the signal versus dose curves for various ions. The amorphous layer formed by the implantation may be a buried layer, in which case it is not the total implanted layer. (This occurs at high implant energies.) At low energies, as in this study, it can be seen that the slope in the plateau region is very near zero. This would indicate that either the amorphous layer width is essentially the same as the implanted layer depth or that, once formed, the amorphous layer width does not increase with dose.

Some discrepancy exists in the determination of the critical dose, especially in the experimental data quoted in Table I from other sources. In these cases the method of determination of the critical dose was usually not well defined. In these cases where the dose curve data were

supplied, a redetermination of the critical dose was made using our method to insure that the same procedure for obtaining the critical dose was used. In all cases the values given in the references were the same as those determined by our method within estimated experimental accuracies.

In comparing our experimental ESR results for 20 keV implants with those reported by a Russian group using electron microscopy for 30 keV implants^{2 5}, good agreement was obtained (Table I). However, in comparing our results with those reported by others⁴ for 200 keV implants using ESR as a tool, discrepancies were found (Table I). Also our experimental data and the data from the Russian group were in good agreement, but the data did not agree well in the case of light ions with the prediction of a previous model for the formation of a continuous amorphous layer in silicon⁴ (see Figure 7).

V. CONCLUSIONS

Because of the discrepancies in the low energy (20-30 keV) data and the high energy (200 keV) data, and the disagreement between the low energy data for light ions and the previous energy independent model, the derivation of the previous model was reconsidered.*

The simple energy independent model for the formation of amorphous silicon by ion implantation at all implant temperatures was formulated by Morehead and Crowder⁴. A summary of their model is as follows: When an ion comes to rest in a crystalline solid, it creates a highly disordered, cylindrical region of many broken bonds and displaced atoms surrounding the ion track. It is then assumed that if all of the target atoms in this region are displaced, the region is amorphous. To create a continuous amorphous layer, the cylindrical regions produced by various ions must overlap. This first occurs when the critical dose, $D(T)$, measured in ions cm^{-2} , has been implanted. This led Morehead and Crowder⁴ to the conclusion that the critical dose at low temperatures, D_0 , was given by

$$D_0 = \bar{E} n_2 \left\langle \frac{dE}{dR} \right\rangle^{-1}, \quad (1)$$

*This conclusion with an appropriate abstract and condensed introduction including Table I and Figure 7 have been accepted for publication in Radiation Effects.

where \bar{E} is the effective energy needed to displace a target atom (≈ 25 eV), n_2 is the number of target atoms per cm^3 , and $\left\langle \frac{dE}{dR} \right\rangle$ is the average energy loss in atomic processes per unit path length. At higher temperatures, defects, probably vacancies, escape by diffusion from the original cylindrical region. Thus the highly disordered region becomes a smaller cylindrical region. Consequently a larger critical dose is required to form a continuous amorphous region. By using a standard exponential temperature dependence for the diffusion coefficient², it was shown that⁴

$$D(T) = D_0 [1 - K' \left\langle \frac{dE}{dR} \right\rangle^{-\frac{1}{2}} \exp(-U/kT)]^2, \quad (2)$$

where the constants K' and U were determined by fitting experimental data, but are also related to defect diffusion properties.

We have reconsidered the derivation of equation (1). This low temperature equation is obtained by assuming that at the critical dose all the energy lost in atomic processes goes into displacing every lattice atom in the amorphous layer. Thus

$$N_1 \left[\left\langle \frac{dE}{dR} \right\rangle W \right] = (n_2 A W_{\perp}) \bar{E}, \quad (3)$$

where N_1 is the total number of incident ions, W is the range of the ions in the amorphous layer, A is the implanted area, and W_{\perp} is the thickness of the amorphous layer perpendicular to the surface. Since $D_0 \equiv N_1/A$, equation (3) yields

$$D_0 = [\bar{E} n_2 \left\langle \frac{dE}{dR} \right\rangle^{-1}] \frac{W_{\perp}}{W}. \quad (4)$$

A rederivation of equation (2) yields

$$D(T) = D_0 \left[1 - K' \left(\left\langle \frac{dE}{dR} \right\rangle \frac{W}{W_{\perp}} \right)^{-\frac{1}{2}} \exp(-U/kT) \right]^2, \quad (5)$$

where D_0 is given in equation (4).

The parameter W_{\perp}/W is a correction factor, as a comparison of equation (1) with equation (4) clearly shows. This factor also modifies both the numerator and denominator of equation (2) as shown in equation (5). Values for W_{\perp}/W can be obtained in the following way. If W_{\perp} is approximately the projected range, then $W_{\perp}/W \approx R_p/R$, where R_p is the range parallel to the incident ion direction and R is the total range of the ion. If, on the other hand, W_{\perp} is small compared to R_p , then $W_{\perp}/W \approx dR_p/dR$. Since $R_p/R \approx dR_p/dR$ (see Reference 3), the actual value of W is not of great importance and the values given for R_p/R in Reference 3 can be used for numerical evaluation of W_{\perp}/W . These values depend on ion energy, ion mass and target atom mass. For a given target, there is a substantial energy dependence for light ions. This is the only energy dependence in equation (5).

Experimental evidence exists which clearly shows an energy dependence in the critical dose for light ions. This evidence is obtained from a compilation of results from three experimental groups: (1) our low energy ESR results; (2) high energy ESR results^{3, 26}; and (3) electron microscope results.²⁵ The data are given in Table I and plotted in Figure 7. Also plotted is the curve for the energy

independent model [equation (2)] and two different energy curves for the energy dependent model [equation (5)]. For all three curves, the previously used⁴ Nielsen approximation and value for U ($= 0.06$ eV) were retained. The old model value of K' [$= 115(\text{keV}/\mu\text{m})^{-\frac{1}{2}}$] was retained for the energy independent curve. For the new model curves, a value of $K' = 126 (\text{keV}/\mu\text{m})^{-\frac{1}{2}}$ was used. The value for K' was changed because

$$K'_{\text{old}} = K'_{\text{new}} (W/W_{\perp})^{-\frac{1}{2}} \quad (6)$$

as a comparison of equation (2) and equation (5) shows. The value for K'_{old} was chosen⁴ by fitting data over which $(W/W_{\perp})^{\frac{1}{2}}$ ranges from about 1.15 to 1.06. As an average value we chose 1.1 and modified K'_{new} accordingly. A somewhat better fit to the data can be obtained by other choices for K' and/or U . However, in order not to obscure the importance of the energy dependent correction, new fitting parameters were not used.

Note that for heavy ions both models agree with the available experimental data. However, for light ions, the low energy data of both N^+ and B^+ show serious disagreement with the old model predictions. The difference in critical dose for the B^+ low energy and high energy data is more than an order of magnitude, and clearly shows a need for an energy dependent model. Figure 7 shows that such a difference is not unexpected in the new, energy dependent model which incorporates the W_{\perp}/W correction factor, even though the old model fitting parameters were used.

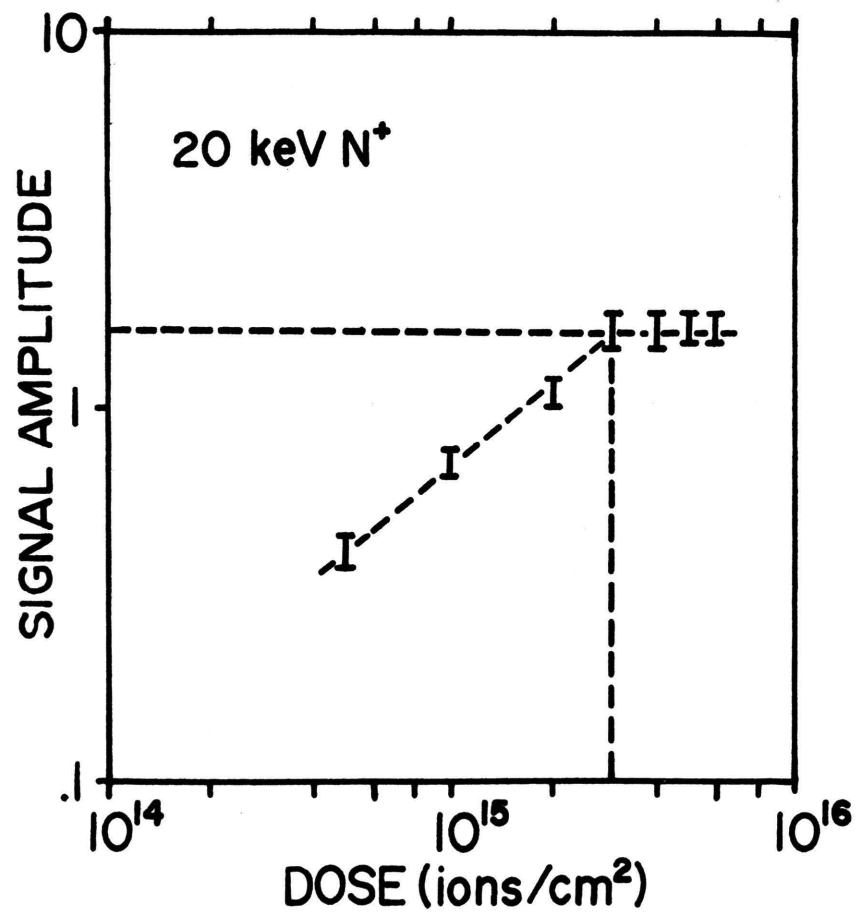


Figure 1. Plot on log-log scale of relative ESR signal amplitude as a function of ion dose for 20 keV N⁺ ions implanted in silicon.

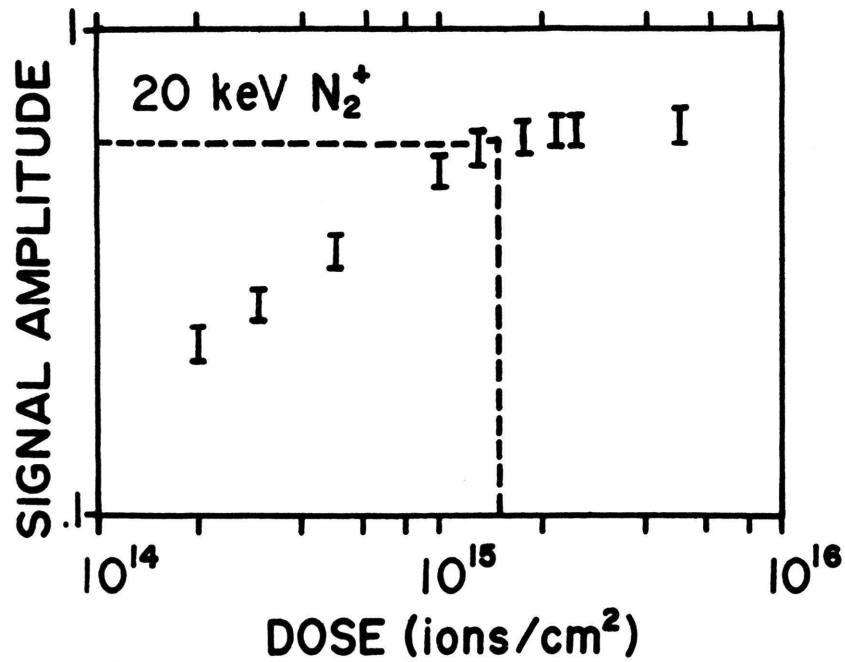


Figure 2. Plot on log-log scale of relative ESR signal amplitude as a function of ion dose for 20 keV N₂⁺ ions implanted in silicon.

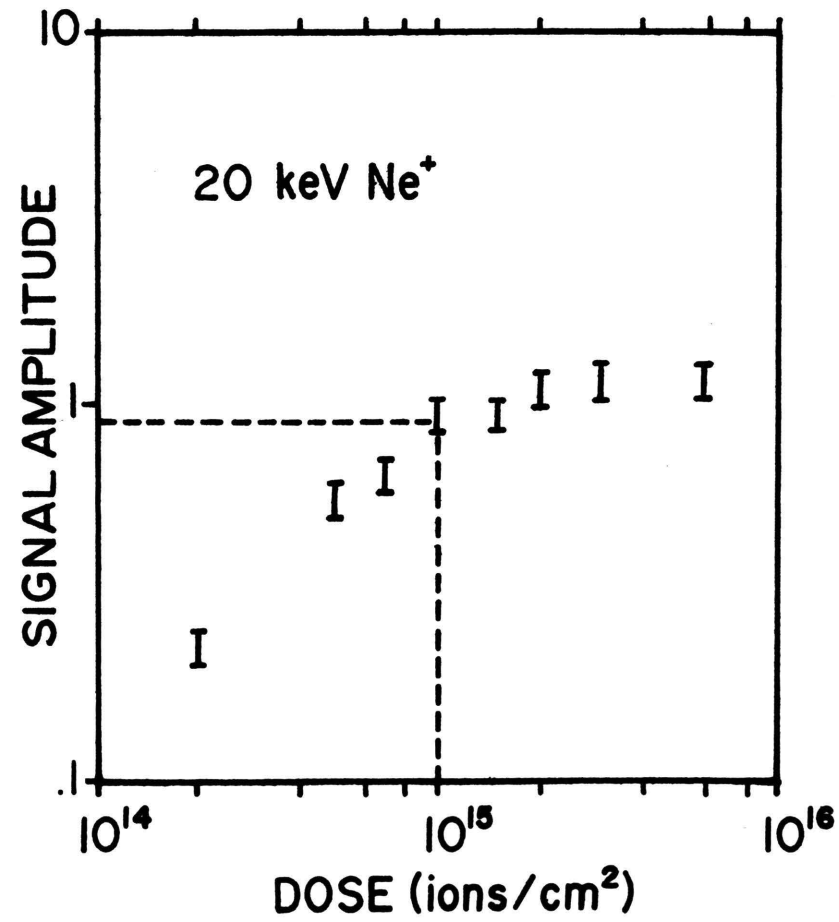


Figure 3. Plot on log-log scale of relative ESR signal amplitude as a function of ion dose for 20 keV Ne⁺ ions implanted in silicon.

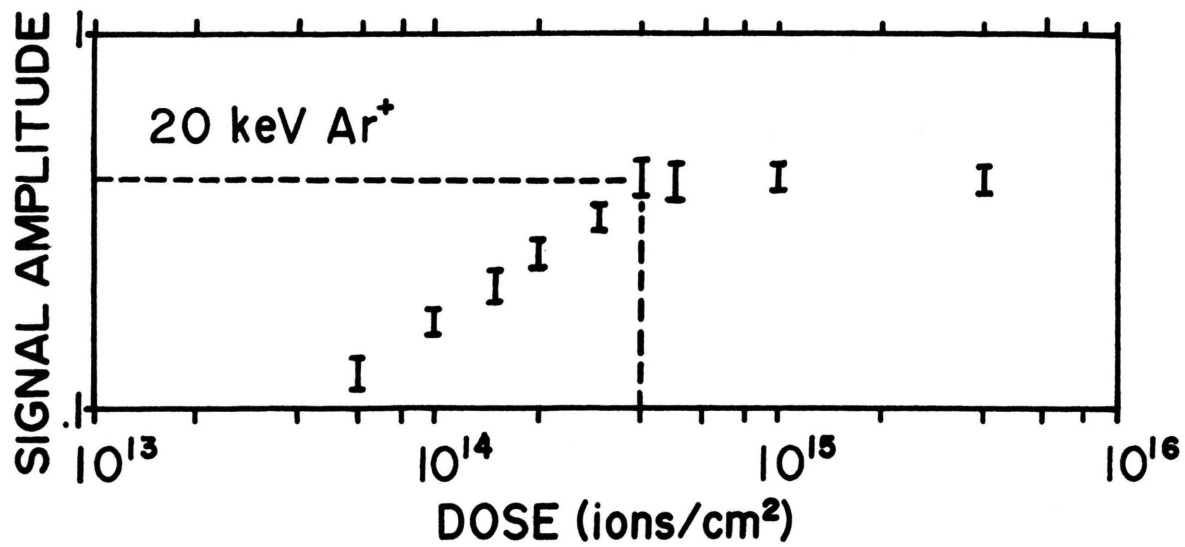


Figure 4. Plot on log-log scale of relative ESR signal amplitude as a function of ion dose for 20 keV Ar⁺ ions implanted in silicon.

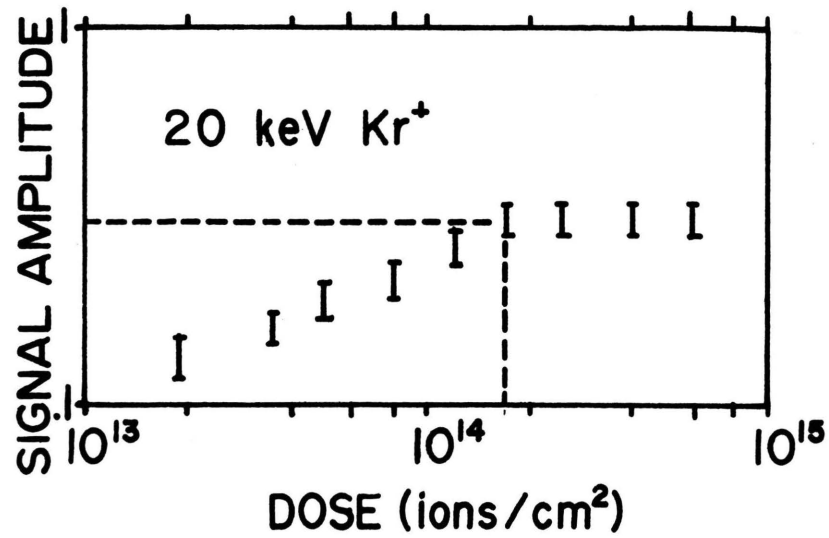


Figure 5. Plot on log-log scale of relative ESR signal amplitude as a function of ion dose for 20 keV Kr⁺ ions implanted in silicon.

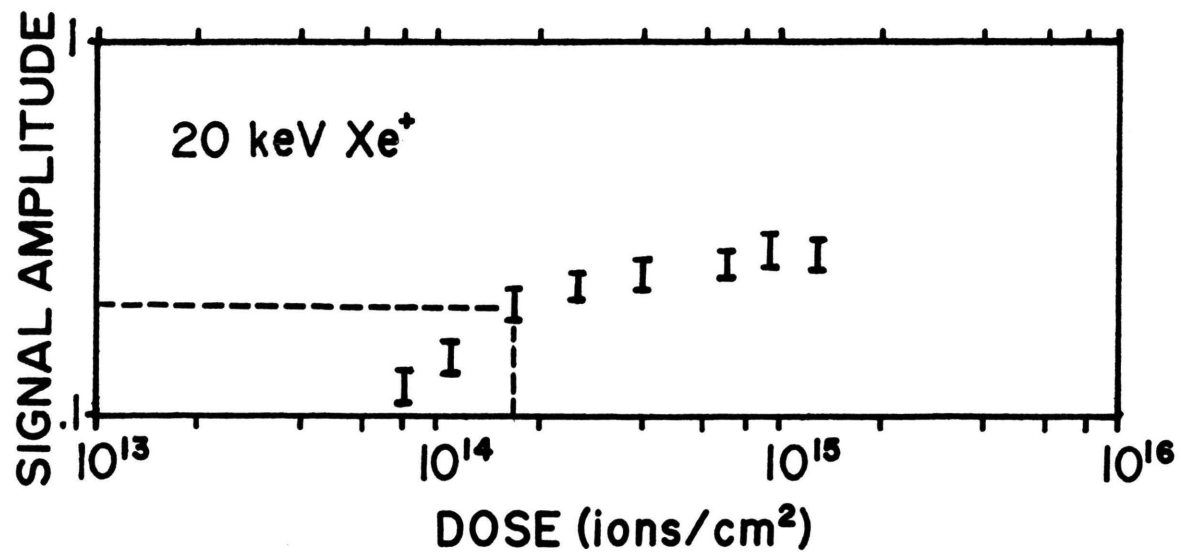


Figure 6. Plot on log-log scale of relative ESR signal amplitude as a function of ion dose for 20 keV Xe⁺ ions implanted in silicon.

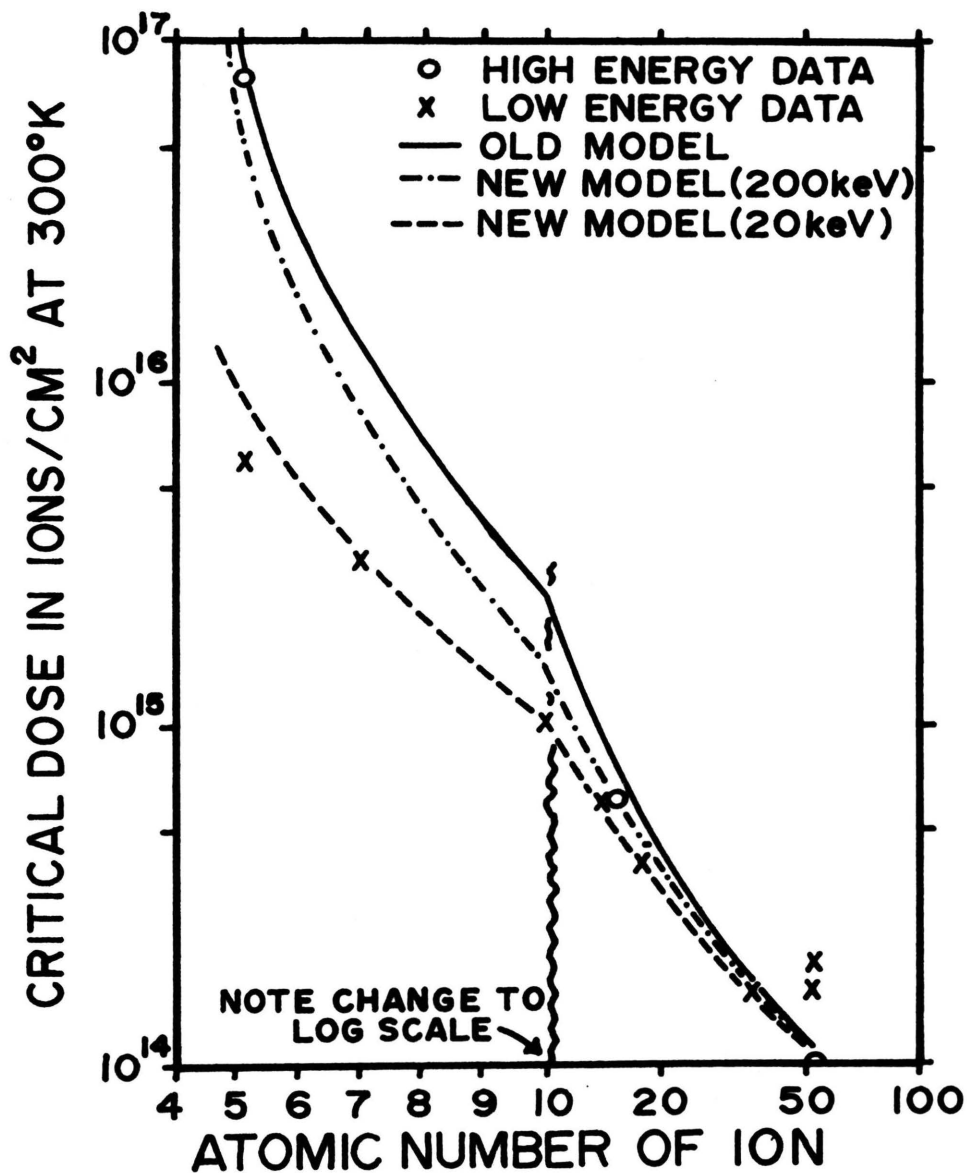


Figure 7. Plot of critical dose at 300°K as a function of atomic number of ion. The solid curve and the two dashed curves are the model curves. The source of the experimental data is given in Table I. Note the change to log scale at $z = 10$ in the abscissa.

TABLE I

Experimentally determined critical dose values for various ions, and energies for room temperature implants.

Ion	Energy in keV	D (300°K) in 10^{16} ions/cm ²	Relative ESR Signal Amplitude
B ⁺	30	0.6 ^a	-
	200	8 ^b	-
N ⁺	20	0.3 ^c	1.6
Ne ⁺	20	0.1 ^c	.96
Si ⁺	30	0.06 ^b	-
P ⁺	30	0.06 ^b	-
	200	0.06 ^b	-
Ar ⁺	20	0.04 ^c	.41
Kr ⁺	20	0.017 ^c	.31
	30	0.017 ^b	-
Sb ⁺	200	0.01 ^a	-
Xe ⁺	20	0.017 ^c	.2
	30	0.02 ^b	-

a See References 4,26.

b See Reference 25.

c This thesis.

BIBLIOGRAPHY

1. J.F. Gibbons, Proc. IEEE 56, 295 (1968).
2. J.F. Gibbons, Proc. IEEE 60, 1062 (1972).
3. J.W. Mayer, L. Eriksson, and J.A. Davies, Ion Implantation in Semiconductors (Academic Press, NY, 1970).
4. F.F. Morehead, Jr. and B.L. Crowder, Rad. Effects 6, 27 (1970).
5. R.S. Ohl, Bell Sys. Tech. J., 31, 104 (1952).
6. W. Shockley, U.S. Patent 2787564.
7. W.D. Cussins, Proc. Phys. Soc. (London), 68, 213 (1955).
8. T. Alvager and N.J. Hansen, Rev. Sci. Instr., 33, 567 (1962).
9. F.M. Rourke, J.C. Sheffield, and F.A. White, Rev. Sci. Instr., 32, 455 (1961).
10. J.O. McCaldin and A.E. Widmer, J. Phys. Chem. Solids, 24, 1073 (1963).
11. J.R. Parsons, Philos. Mag., 12, 1159 (1965).
12. J.A. Davies, J. Denhartog, L. Eriksson, and J.W. Mayer, Can. J. Phys., 45, 4053 (1967).
13. J.W. Mayer, L. Eriksson, S.T. Picraux, and J.A. Davies, Can. J. Phys., 46, 663 (1968).
14. D.F. Daly, Appl. Phys. Letters, 15, 267 (1969).
15. K.L. Brower, F.L. Vook, and J.A. Borders, Appl. Phys. Letters, 16, 108 (1970).
16. K.L. Brower and J.A. Borders, Appl. Phys. Letters, 16, 169 (1970).
17. K.L. Brower and W. Beezhold, J. Appl. Phys. 43, 3499 (1972).
18. H. Sugimoto, Y. Shiraki, and K.F. Komatsubara, Appl. Phys. Letters, 18, 461 (1971).
19. S. Hasegawa, R. Kontani, and T. Shimizu, Jap. J. Appl. Phys, 10, 655 (1971).

20. B.L. Crowder and R.S. Title, Rad. Effects, 6, 63 (1970).
21. G.D. Watkins, Proc. Santa Fe Conf. on Rad. Effects in Semiconductors, Santa Fe, N.M., (1967).
22. S.C. Agarwal, Phys. Rev. B, 1, 685 (1973).
23. M.H. Brodsky and R.S. Title, Phys. Rev. Letters, 23, 581 (1969).
24. B.L. Crowder, R.S. Title, M.H. Brodsky, and G.D. Pettit, Appl. Phys. Letters, 16, 205 (1970).
25. V.M. Gusev, Yu. V. Martynenko, and K.V. Starinin, Soviet Phys. - Cry., 14, 908 (1970).
26. F.F. Morehead, B.L. Crowder, and R.S. Title, J. Appl. Phys. 43, 1112 (1972).

VITA

John Robert Dennis was born in Browning, Missouri on January 20, 1943. His first three years of primary education was received in a one room country school in Linn County, Missouri. The remainder of his primary and secondary education was obtained in Meadville, Missouri. After graduation from high school in 1961 he attended Northeast Missouri State Teachers College for one year.

In 1962 he was employed by a retail lumber and hardware company in Chillicothe, Missouri and later in Breckenridge, Missouri. He resigned his position in 1967 to attend the University of Missouri-Rolla where he obtained his Bachelor of Science degree in Physics in May, 1971. Since that time he has been enrolled in the Graduate School of the University of Missouri-Rolla.